Acta Crystallographica Section E
Structure Reports Online
ISSN 1600-5368

Rietveld refinement of Y_2GeO_5

Eric M. Rivera-Muñoz[a]* and Lauro Bucio[b]

[a]Centro de Física Aplicada y Tecnología Avanzada, Universidad Nacional Autónoma de México, AP 1-1010, Queretaro, Qro. 76000, Mexico, and [b]Instituto de Física, Universidad Nacional Autónoma de México, AP 20-364, 01000 México DF, Mexico
Correspondence e-mail: emrivera@fata.unam.mx

Received 25 June 2009; accepted 8 July 2009

Key indicators: powder X-ray study; T = 300 K; mean σ(Y–O) = 0.009 Å; R factor = 0.053; wR factor = 0.069; data-to-parameter ratio = 5.5.

Y_2GeO_5 (yttrium germanium pentaoxide) was synthesized by solid-state reaction at 1443 K. The arrangement, which has monoclinic symmetry, is isostructural with Dy_2GeO_5 and presents two independent sites for the Y atoms. Around these atoms there are distorted six-coordinated YO_6 octahedra and seven-coordinated YO_7 pentagonal bipyramids. The YO_7 polyhedra are linked together, sharing their edges along a surface parallel to *ab*, forming a sheet. Each of these parallel sheets is interconnected by means of GeO_4 tetrahedra, sharing an edge (or vertex) on one side and a vertex (or edge) on the other adjacent side. Parallel sheets of YO_7 polyhedra are also interconnected by undulating chains of YO_6 octahedra along the *c* axis. These octahedra are joined together, sharing a common edge, to form the chain and share edges with the YO_7 polyhedra of the sheets.

Related literature

For the isotypic structure of Dy_2GeO_5, see: Brixner *et al.* (1985). Different synthesis methods have been reported for this compound, including preparation by conventional r.f. magnetron sputtering (Minami *et al.*, 2003), solid-state reactions at high temperatures (Zhao *et al.*, 2003), MOCVD and LSMCD (Natori *et al.*, 2004). For bond-valence parameters, see: Brese & O'Keeffe (1991), and for the bond-valence model, see: Brown (1981, 1992). For oxide phosphors, see: Minami *et al.* (2001, 2002, 2004). Data used to model the second phase present in the reaction product, $Y_2Ge_2O_7$, were taken from Redhammer *et al.* (2007). For related literature on technological applications, see: Fei *et al.* (2003).

Experimental

Crystal data

Y_2GeO_5
M_r = 330.43
Monoclinic, $I2/a$
a = 10.4706 (2) Å
b = 6.8292 (1) Å
c = 12.8795 (2) Å
β = 101.750 (3)°
V = 901.66 (3) Å^3
Z = 8
Cu $K\alpha$ radiation
T = 300 K
Specimen shape: flat sheet
20 × 20 × 0.2 mm
Specimen prepared at 1443 K
Particle morphology: spherical, white

Data collection

Bruker Advance D8 diffractometer
Specimen mounting: packed powder sample container
Specimen mounted in reflection mode
Scan method: step
$2\theta_{min}$ = 8.0, $2\theta_{max}$ = 80.0°
Increment in 2θ = 0.02°

Refinement

R_p = 0.053
R_{wp} = 0.069
R_{exp} = 0.024
S = 2.90
Wavelength of incident radiation: 1.540560 Å
Profile function: pseudo-Voigt modified by Thompson *et al.* (1987)
582 reflections
105 parameters

Data collection: *DIFFRAC/AT* (Siemens, 1993); cell refinement: *DICVOL91* (Boultif & Louër 1991); data reduction: *FULLPROF* (Rodríguez-Carvajal, 2006); method used to solve structure: coordinates taken from an isotypic compound (Brixner *et al.*, 1985); program(s) used to refine structure: *FULLPROF*; molecular graphics: *ATOMS* (Dowty, 2000); software used to prepare material for publication: *FULLPROF*.

The authors acknowledge the collaboration of Manuel Aguilar Franco for performing the conventional X-ray diffraction measurements, and projects CONACyT SEP-2007–81700.

Supplementary data and figures for this paper are available from the IUCr electronic archives (Reference: BR2110).

References

Boultif, A. & Louër, D. (1991). *J. Appl. Cryst.* **24**, 987–993.
Brese, N. E. & O'Keeffe, M. (1991). *Acta Cryst.* B**47**, 192–197.
Brixner, L. H., Calabrese, J. C. & Chen, H.-Y. (1985). *J. Less-Common Met.* **110**, 397-410.
Brown, I. D. (1981). *Structure and Bonding in Crystals*, Vol. 2, edited by M. O'Keefe & A. Navrotsky, pp. 1–30. New York: Academic Press.
Brown, I. D. (1992). *Z. Kristallogr.* **199**, 255–272.
Dowty, E. (2000). *ATOMS for Windows*. Shape Software, Kingsport, Tennessee, USA.
Fei, Z., Peimin, G., Guobao, L., Fuhui, L., Shujian, T. & Xiping, J. (2003). *Mater. Res. Bull.* **38**, 931–940.
Minami, T., Kobayashi, Y., Miyata, T. & Yamazaki, M. (2003). *Thin Solid Films*, **425**, 35–40.
Minami, T., Miyata, T., Ueno, T. & Urano, Y. (2002). US Patent No. 2002/0047515 Al.
Minami, T., Miyata, T., Ueno, T. & Urano, Y. (2004). US Patent No. 6707249 B2.
Minami, T., Yamazaki, M., Miyata, T. & Shirai, T. (2001). *Jpn J. Appl. Phys.* **40**, L864–L866.
Natori, E., Kijima, T., Furuyama, K. & Tasaki, Y. (2004). Eur. Patent No. EP20020738688.
Redhammer, G. J., Roth, G. & Amthauer, G. (2007). *Acta Cryst.* C**63**, i93–i95.
Rodríguez-Carvajal, J. (2006). *FULLPROF*. URL: http://www.ill.eu/sites/fullprof/ php/reference.html.
Siemens (1993). *DIFFRAC/AT*. Siemens Analytical X-ray Instruments Inc., Madison, Wisconsin, USA.
Thompson, P., Cox, D. E. & Hastings, J. B. (1987). *J. Appl. Cryst.* **20**, 79–83.
Zhao, F., Guo, P., Li, G., Liao, F., Tian, S. & Jing, X. (2003). *Mater. Res. Bull.* **38**, 931–940.

supplementary materials

Acta Cryst. (2009). E**65**, i60 [**doi:10.1107/S1600536809026579**]

Rietveld refinement of Y_2GeO_5

E. M. Rivera-Muñoz and L. Bucio

Comment

Field emission display (FED) constitutes the next generation of information display devices. Its advantages include portable size with low power consumption, broad viewing angle, and wide operating-temperature range among others (Zhao *et al.*, 2003). New multicomponent oxide phosphor, Mn-activated Y_2O_3—GeO_2, is promising as the thin-film emitting layer for thin-film electroluminescent (TFEL) devices (Minami *et al.*, 2001). The oxide phosphor for use in those electroluminescent devices is formed from yttrium oxide and a transition metal as an activator, or from Y—Ge—O oxide and one metallic element to form *M*:Y_2GeO_5 where *M* is a metal (Minami *et al.*, 2002; Minami *et al.*, 2004). Other reported use for Y_2GeO_5 consists in piezoelectric ceramics in the form of films which include a complex oxide material having an oxygen octahedral structure and a paraelectric material having a catalytic effect for the complex oxide material in a mixed state. Paraelectric material could be a layered compound having an oxygen tetrahedral structure which includes one compound with the form $MSiO_x$ (*M*=metal) and Y_2GeO_5 (Natori *et al.*, 2004). Fig. 1a show a fragment of the crystal structure of Y_2GeO_5 along the *ab* plane in which YO_7 polyhedra share common edges forming a mesh. These YO_7 polyhedra are represented as medium slate blue. Over the mesh, there are isolated GeO_4 tetrahedra, which are represented in yellow in Fig. 1a. Each one of these parallel sheets are interconnected by means of GeO_4 tetrahedra, sharing an edge (or vertix) in one side and a vertix (or edge) in the other adjacent side respectively as can be seen in Fig. 1b. Undulating chains of YO_6 octahedra along the *c* axis are represented in gray in Fig. 1c in which the YO_7 polyhedra were not represented in order lo clarify this feature of the arrangement. The chains of YO_6 octahedra also interconnect the parallel sheets of YO_7 polyhedra, as can be see in the unit cell of Y_2GeO_5 represented in Fig. 1d. Bond valence calculations were made using the recommended bond-valence parameters for oxides published by Brese & O'Keeffe (1991). Bond valence sum (BVS) around six-coordinated Y1, seven-coordinated Y2, and Ge give the values of 3.03, 2.76 and 4.08 respectively, being the first and the last closer to the values of +3 and +4 expected for the yttrium and germanium atoms respectively. The second value of 2.76 was first interpreted as stretched bonds around Y2 exist, but this suggestion was withdrawn because there is no compressed cation in the unit cell capable to balance the supposed stretched bonds around Y2, as it is established in the Brown's bond valence model (Brown, 1981) for evaluating the existence of stresses in the crystal. In fact, calculating the so called *Global Instability Index*, which is obtained as the root mean square of the bond-valence sum deviation for all the N atoms present in the asymmetric unit (Brown, 1992) a value of 0.06 was obtained suggesting no strain. This is a remarkably low value for a Rietveld refinement (for a well refined and unstrained structure this is less than 0.1). Then, the low value of the bond valence sum around Y2 is well within normal limits for a Rietveld refinment where larger deviations are typically found.

Experimental

The reactive mixture was prepared from Y_2O_3 (Aldrich.99.99%) and GeO_2 (CERAC 99.999%) according to the stoichiometric proportions desired. The mixture was first powdered using an agate mortar; and then was heated in air in a tube furnace at 1373 K for 5 days with intermediate regrindings. A second thermal treatment at 1443 K for two days was applied. The characterization of the bulk material by conventional X-ray powder diffraction data indicated the presence of a well crys-

tallized phase showing reflections that match with the isostructural phase $DyGeO_5$ (PDF 01–078–0478). Very small amount of a secondary phase $Y_2Ge_2O_7$ (PDF 38–288) was identified.

Refinement

The starting structural parameters for perform a Rietveld refinement of the Y_2GeO_5 phase were taken from the isostructural data reported for Dy_2GeO_5 (ICSD 61373) by Brixner *et al.* (1985). For modeling the second phase $Y_2Ge_2O_7$ (ICSD 240989), the data were those reported by Redhammer *et al.* (2007). The following parameters were refined: zero point and scale factors, cell parameters, half-width profile parameters, overall temperature factors, atomic coordinates, and asymmetries. For the $Y_2Ge_2O_7$ phase the atomic coordinates were fixed to their starting values. The final Rietveld refinement of conventional diffraction pattern is shown in Fig. 2.

Figures

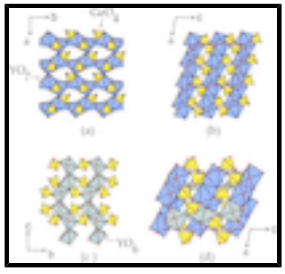

Fig. 1. (*a*) View of a YO_7 layer in the Y_2GeO_5 structure (*ab* projection). YO_7 polyhedra are represented in medium slate blue while GeO_4 tetrahedra are represented in yellow. (*b*) View of the Y_2GeO_5 structure (*ac* projection). The layers formed by YO_7 polyhedra are linked together by GeO_4 tetrahedra. (*c*) Chains of YO_6 octahedra (in gray) undulating along the *c* axis sharing common edges and linked with other chains by mean of GeO_4 tetrahedra. (*d*) Unit cell for Y_2GeO_5 structure.

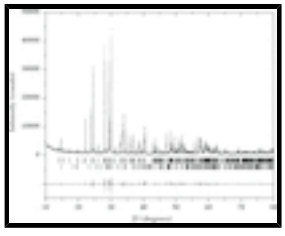

Fig. 2. Rietveld refinement for X-ray diffraction data. Observed (crosses), calculated (solid line) and difference (bottom trace) plots are represented; vertical marks correspond to the allowed Bragg reflections for Y_2GeO_5 (top) and $Y_2Ge_2O_7$ (bottom) as secondary phase.

yttrium germanium pentaoxide

Crystal data

$Y_2Ge_1O_5$	$Z = 8$
$M_r = 330.43$	$F_{000} = 1200$
Monoclinic, *I*2/*a*	$D_x = 4.868$ Mg m^{-3}
Hall symbol: -I 2ya	Cu *K*α radiation, λ = 1.540560 Å
$a = 10.4706$ (2) Å	$T = 300$ K
$b = 6.8292$ (1) Å	Specimen form: flat sheet; particle morphology spherical; white
$c = 12.8795$ (2) Å	20 × 20 × 0.2 mm
β = 101.750 (3)º	Specimen preparation: temperature 1443 K
$V = 901.66$ (3) Å^3	

Data collection

Bruker Advance D8 diffractometer	Scan method: step
Monochromator: graphite	T = 300 K
Specimen mounting: packed powder sample container	$2\theta_{min}$ = 8.00, $2\theta_{max}$ = 80.02º
Specimen mounted in reflection mode	Increment in 2θ = 0.02º

Refinement

Least-squares matrix: full with fixed elements per cycle	Profile function: pseudo-Voigt modified by Thompson *et al.* (1987)
R_p = 0.053	105 parameters
R_{wp} = 0.069	Weighting scheme based on measured s.u.'s ?
R_{exp} = 0.024	$(\Delta/\sigma)_{max}$ = 0.02
S = 2.90	Extinction coefficient: ?

Fractional atomic coordinates and isotropic or equivalent isotropic displacement parameters (Å^2)

	x	*y*	*z*	U_{iso}*/U_{eq}
Y1	0.3011 (2)	0.6277 (2)	0.6380 (1)	0.0096 (7)
Y2	0.0708 (2)	0.2567 (3)	0.5355 (1)	0.0090 (7)
Ge1	0.6236 (2)	0.5933 (3)	0.8155 (2)	0.0121 (9)
O1	0.1210 (9)	0.604 (1)	0.5178 (8)	0.009 (2)
O2	0.2950 (9)	0.298 (1)	0.6172 (7)	0.009 (2)
O3	0.5212 (9)	0.654 (1)	0.6971 (8)	0.009 (2)
O4	0.551 (1)	−0.006 (1)	0.4155 (8)	0.009 (2)
O5	0.2412 (8)	0.572 (1)	0.7926 (8)	0.009 (2)

Geometric parameters (Å, °)

Y1—O1	2.189 (8)	Y2—O2^{i}	2.655 (10)
Y1—O1^{i}	2.321 (10)	Y2—O3^{iv}	2.327 (10)
Y1—O2	2.270 (8)	Y2—O4^{i}	2.358 (9)
Y1—O3	2.283 (8)	Y2—O4^{v}	2.287 (9)
Y1—O5	2.238 (10)	Ge1—O2^{vi}	1.767 (8)
Y1—O5^{ii}	2.316 (8)	Ge1—O3	1.727 (8)
Y2—O1	2.447 (8)	Ge1—O4^{vii}	1.732 (10)
Y2—O1^{iii}	2.203 (8)	Ge1—O5^{viii}	1.739 (9)
Y2—O2	2.386 (8)		
Y1—O1—Y1^{ix}	53.6 (2)	Y1—O2—Y2^{xiii}	118.8 (3)
Y1—O1—Y2^{x}	128.7 (3)	Y2^{xii}—O2—Y2^{xiii}	61.19 (6)
Y1^{ix}—O1—Y2^{x}	78.64 (6)	Y1—O3—Y2^{xiv}	110.7 (3)
Y1^{ix}—O1—Y2^{xi}	90.44 (7)	Y2^{xv}—O4—Y2^{xvi}	124.20 (7)
Y2^{x}—O1—Y2^{xi}	157.05 (6)	Y1—O5—Y1^{xvii}	89.8 (2)

Y1—O2—Y2^{xii}	97.4 (2)

Symmetry codes: (i) −*x*+1/2, *y*, −*z*+1; (ii) −*x*+1/2, −*y*+3/2, −*z*+3/2; (iii) −*x*, −*y*+1, −*z*+1; (iv) *x*−1/2, −*y*+1, *z*; (v) *x*−1/2, −*y*, *z*; (vi) −*x*+1, *y*+1/2, −*z*+3/2; (vii) *x*, −*y*+1/2, *z*+1/2; (viii) *x*+1/2, −*y*+1, *z*; (ix) −*x*+3/2, *y*, −*z*+1; (x) −*x*, −*y*, −*z*; (xi) *x*+1/2, −*y*+1, *z*+1; (xii) −*x*+1/2, *y*, −*z*; (xiii) −*x*+1, −*y*, −*z*+1; (xiv) −*x*+3/2, *y*+1, −*z*; (xv) *x*+1, *y*, *z*+1; (xvi) −*x*+3/2, *y*, −*z*; (xvii) −*x*+3/2, *y*+2, −*z*+2.

Fig. 1

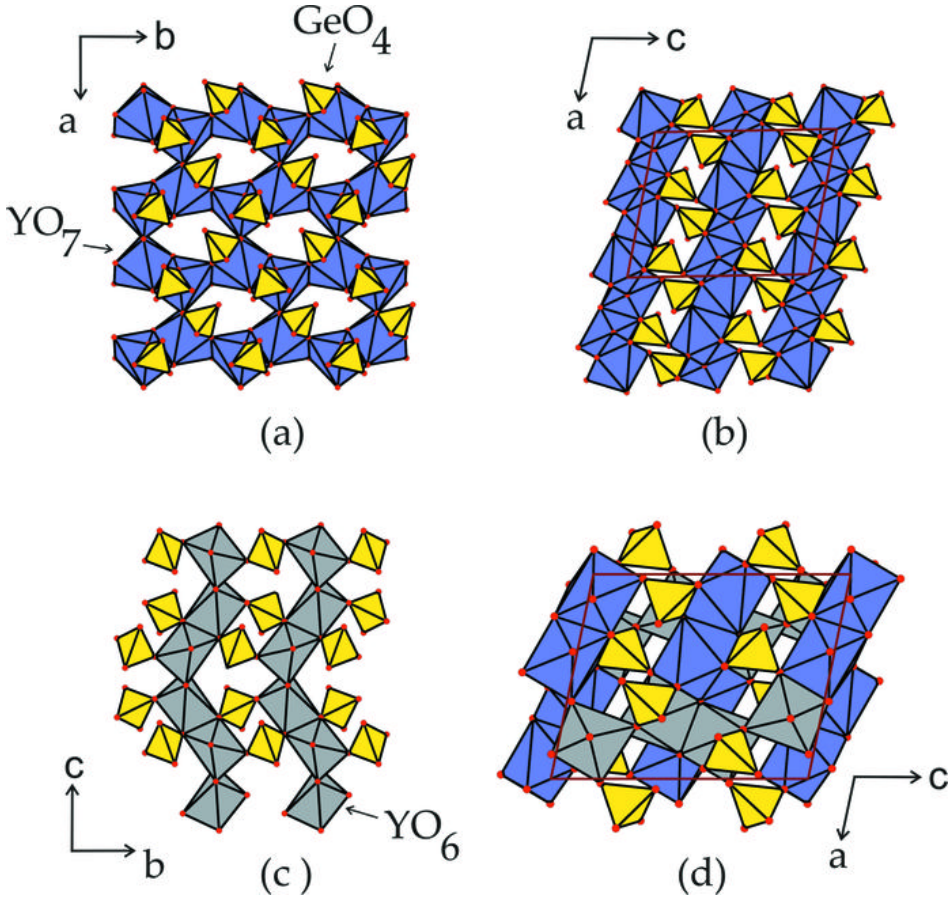

Fig. 2

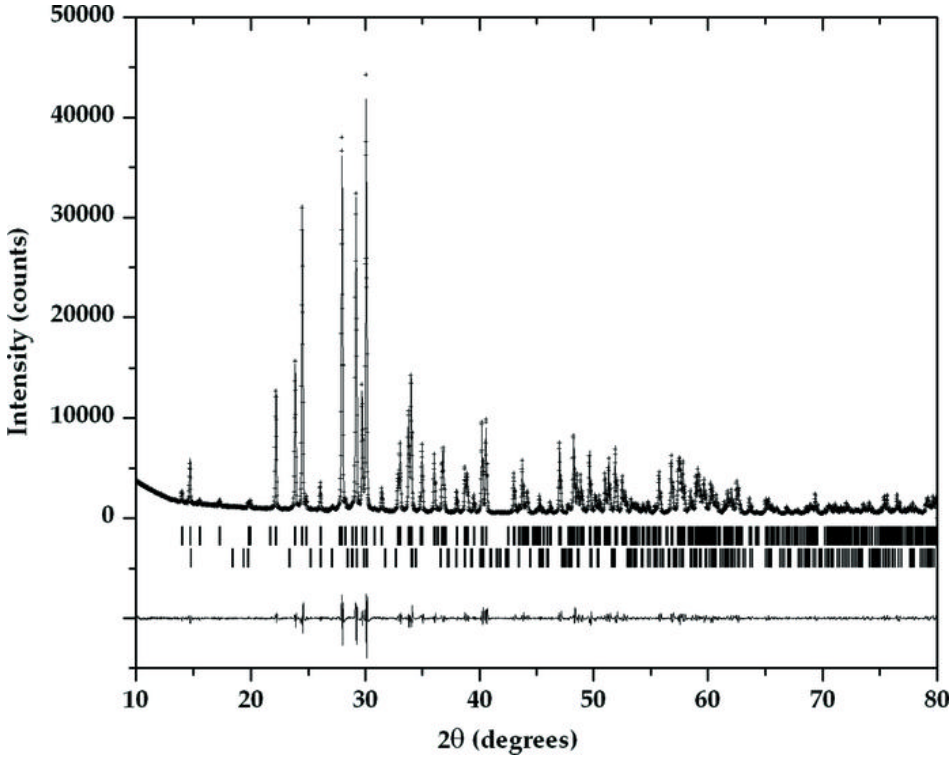
50000
40000
30000
20000
10000
0
Intensity (counts)
10
20
30
40
50
60
70
80
2θ (degrees)